Eur. Phys. J. A **22**, 481–487 (2004)
DOI 10.1140/epja/i2003-10240-x

THE EUROPEAN PHYSICAL JOURNAL A

Strange and singlet form factors of the nucleon: Predictions for G0, A4, and HAPPEX II experiments

A. Silva[1,2,a], H.-Ch. Kim[3,b], and K. Goeke[1,c]

[1] Institut für Theoretische Physik II, Ruhr-Universität Bochum, D-44780 Bochum, Germany
[2] Departamento de Física and Centro de Física Computacional, Universidade de Coimbra, P-3000 Coimbra, Portugal
[3] Department of Physics, Nuclear Physics & Radiation Technology Institute (NuRI), Pusan National University, 609-735 Busan, Republic of Korea

Received: 27 August 2003 / Revised version: 28 May 2004 /
Published online: 11 November 2004 –
Communicated by U.-G. Meißner

Abstract. We investigate the strange and flavor-singlet electric and magnetic form factors of the nucleon within the framework of the $SU(3)$ chiral quark-soliton model. Isospin symmetry is assumed and the symmetry-conserving $SU(3)$ quantization is employed, rotational and strange-quark mass corrections being included. For the experiments G0, A4, and HAPPEX II we predict the quantities $G_E^0+\beta G_M^0$ and $G_E^{\rm s}+\beta G_M^{\rm s}$. The dependence of the results on the parameters of the model and the treatment of the Yukawa asymptotic behavior of the soliton are investigated.

PACS. 12.40.-y Other models for strong interactions – 14.20.Dh Protons and neutrons

1 Introduction

It is of utmost importance to understand the strangeness content of the nucleon, since it gives a clue about its internal quark structure. In particular, the deviation from the valence quark picture and the polarization of the quark sea must be investigated. In fact, with this aim a great deal of experimental and theoretical effort has been put into the study of the strangeness in the nucleon in various channels: The spin content of the nucleon [1–5], the πN sigma term $\Sigma_{\pi\rm N}$ [6], and the strange vector form factors [7,8]. In particular, the strange vector form factors have been a hot issue recently, as their first measurement was achieved by the SAMPLE Collaboration [9–11] at MIT/Bates, parity-violating electron scattering being used. The most recent result by the SAMPLE Collaboration [11] for the strange magnetic form factor finds (Q^2 in (GeV/c)^2)

$$G_M^{\rm s}(Q^2=0.1) = (+0.14 \pm 0.29\,({\rm stat.}) \pm 0.31\,({\rm syst.}))\,{\rm n.m.} \tag{1}$$

It is extracted from the knowledge of both the neutral weak magnetic form factor G_M^Z measured in parity-violating elastic e-p scattering and the electromagnetic form factors $G_M^{{\rm p}\gamma}$, $G_M^{{\rm n}\gamma}$ by using the relation (assuming isospin invariance)

$$G_M^Z = \left(1-4\sin^2\theta_{\rm W}\right) G_M^{{\rm p}\gamma} - G_M^{{\rm n}\gamma} - G_M^s\,, \tag{2}$$

where $\theta_{\rm W}$ is the Weinberg mixing angle determined experimentally [12]: $\sin^2\theta_{\rm W} = 0.23147$.

The HAPPEX Collaboration at TJNAF also announced the measurement of the strange vector form factors [13]. The asymmetry $A_{\rm th}$ is obtained from the parity-violating polarized electron scattering, from which the singlet form factors are extracted:

$$\frac{(G_E^0+0.392G_M^0)}{(G_M^{{\rm p}\gamma}/\mu_{\rm p})}(Q^2=0.477) = 1.527 \pm 0.048 \pm 0.027 \pm 0.011. \tag{3}$$

With the help of the available data for the electromagnetic form factors via the relation

$$G_{E,M}^{\rm s} = G_{E,M}^0 - G_{E,M}^{{\rm p}\gamma} - G_{E,M}^{{\rm n}\gamma}, \tag{4}$$

the HAPPEX Collaboration arrives at the following result about the strange form factors:

$$(G_E^{\rm s}+0.392G_M^{\rm s})(Q^2=0.477) = 0.025\pm0.020\pm0.014, \tag{5}$$

where the first error is experimental and the second one is from the uncertainties in electromagnetic form factors.

There has been a great deal of theoretical effort in order to predict the strange vector form factors [14] and

[a] e-mail: ajose@teor.fis.uc.pt
[b] e-mail: hchkim@pusan.ac.kr
[c] e-mail: Klaus.Goeke@tp2.ruhr-uni-bochum.de

each approach emphasizes different aspects. Beck, Holstein, and McKeown reviewed some of theoretical works in refs. [15, 16].

A proper theoretical description of the strange form factors of the nucleon should be based on QCD. Since, however, these form factors basically reflect the excitation of $s\bar{s}$ pairs, it is very difficult to use lattice gauge techniques because they are still hampered by technical problems, in particular, with light quarks. Thus, appropriate models are required, which are based on QCD and treat the relevant degrees of freedom in a good approximation. One of those is the chiral quark-soliton model (χQSM). It is an effective quark theory of the instanton degrees of freedom of the QCD vacuum and results in a Lagrangian for valence and sea quarks both moving in a static self-consistent Goldstone background field [17, 18]. It has successfully been applied to electromagnetic and axial-vector form factors [17] and to forward and generalized parton distributions [19–21] and has lead even to the prediction of the heavily discussed pentaquark baryon Θ^+ [22].

Two of the present authors studied the strange vector form factors within the framework of this χQSM some years ago [23]. The formalism used contains a conceptual difficulty because the rotational corrections break the venerable Gell-Mann-Nishijima relation [24]. The reason for this lies probably in the fact that the large N_c expansion, underlying the stationary phase approximation of the χQSM, has not been fully extended to the $SU(3)$ collective quantization procedure. Instead, Praszałowicz *et al.* [25] suggested on practical grounds an approximate formalism, which fulfills the Gell-Mann-Nishijima relation and in addition has proper limits for large and small solitonic radii, *i.e.* the limit of the Sykrme model and the nonrelativistic quark model, respectively. This so-called symmetry-conserving quantization method [25] is used in the present paper and the corresponding formulae, thereby correcting also a technical error of ref. [23], are given in the appendix.

The present authors have recently reinvestigated the strange vector form factors, following the above-mentioned quantization scheme of Praszałowicz *et al.* [25]. We presented some aspects of the SAMPLE, HAPPEX, and A4 experiments within the framework of the χQSM [26]. Results have shown a fairly good agreement with experimental data of the SAMPLE and HAPPEX. In this work, we want to extend the former investigation, to document the relevant formulae of the model and to present the results pertinent to future experiments: G0 experiments being conducted at TJNAF will measure a linear combination of the strange vector form factors at seven different values of the momentum transfer Q^2 with two different angles, *i.e.* the forward angle $\theta = 10°$ and the backward angle 108°. With these measurements, the strange electric and magnetic form factors can be separately obtained. The A4 experiment at MAMI will soon bring out the new data at $Q^2 = 0.227\ \text{GeV}^2$ with $\theta = 35°$ [27]. The planned HAPPEX II experiment will measure the combination of the strange vector form factors at $Q^2 = 0.11\ \text{GeV}^2$, which is the same momentum transfer as the SAMPLE experiment, with the forward angle $\theta = 6°$ to extract the separated strange electric and magnetic form factors with the SAMPLE data combined. Thus, in the present work, we will continue our previous work [26] and will concentrate on predicting the above-given future experiments, in particular, G0 experiment.

2 Strange and singlet vector form factors

In this section we very briefly review the formalism of the χQSM. Details of the model [28] can be found in ref. [17]. Employing in the following the non-standard sign convention used by Jaffe [7] for the strange vector current, the strange and singlet vector form factors of the baryons are expressed in the quark matrix elements as follows:

$$\langle N(p')|J_\mu^{\mathrm{s},(0)}|N(p)\rangle = \bar{u}_{\mathrm{N}}(p') \times \left[\gamma_\mu F_1^{\mathrm{s},0}(q^2) + i\sigma_{\mu\nu}\frac{q^\nu}{2M_{\mathrm{N}}}F_2^{\mathrm{s},0}(q^2)\right]u_{\mathrm{N}}(p), \quad (6)$$

where q^2 is the square of the four-momentum transfer $q^2 = -Q^2$ with $Q^2 > 0$. M_{N} and $u_{\mathrm{N}}(p)$ stand for the nucleon mass and its spinor, respectively. The strange-quark current J_μ^{s} can be expressed in terms of the flavor-singlet and flavor-octet currents in Euclidean space:

$$J_\mu^{\mathrm{s}} = -i\psi^\dagger\gamma_\mu\hat{Q}_{\mathrm{s}}\psi = \frac{1}{N_c}J_\mu^{(0)} - \frac{1}{\sqrt{3}}J_\mu^{(8)}, \quad (7)$$

where $J_\mu^{(0)}$ and $J_\mu^{(8)}$ are the flavor-singlet and flavor-octet currents, respectively:

$$J_\mu^{(0)} = -i\psi^\dagger\gamma_\mu\psi\,, \qquad J_\mu^{(8)} = -i\psi^\dagger\gamma_\mu\lambda_8\psi\,. \quad (8)$$

Here, $N_c = 3$ is correctly introduced to make it sure that the baryon number is equal to unity. The baryon and hypercharge currents are equal to the singlet and octet currents, respectively.

The strange (singlet) Dirac form factors $F_1^{\mathrm{s},0}$ and $F_2^{\mathrm{s},0}$ can be written in terms of the strange (singlet) Sachs form factors, $G_E^{\mathrm{s},0}(Q^2)$ and $G_M^{\mathrm{s},0}(Q^2)$:

$$G_E^{\mathrm{s},0}(Q^2) = F_1^{\mathrm{s},0}(Q^2) - \frac{Q^2}{4M_{\mathrm{N}}^2}F_2^{\mathrm{s},0}(Q^2)\,, \qquad G_M^{\mathrm{s},0}(Q^2) = F_1^{\mathrm{s},0}(Q^2) + F_2^{\mathrm{s},0}(Q^2)\,. \quad (9)$$

Having carried out a lengthy calculation following strictly refs. [25, 29], we obtain the expressions for the strange vector form factors and flavor-singlet form factors of the nucleon:

$$G_E^{\mathrm{s},0}(\boldsymbol{Q}^2) = G_E^{\mathrm{s},0,m_{\mathrm{s}}^0}(\boldsymbol{Q}^2) + G_E^{\mathrm{s},0,m_{\mathrm{s}}^1,\mathrm{op}}(\boldsymbol{Q}^2) + G_E^{\mathrm{s},0,m_{\mathrm{s}}^1,\mathrm{wf}}(\boldsymbol{Q}^2),$$
$$G_M^{\mathrm{s},0}(\boldsymbol{Q}^2) = G_M^{\mathrm{s},0,m_{\mathrm{s}}^0}(\boldsymbol{Q}^2) + G_M^{\mathrm{s},0,m_{\mathrm{s}}^1,\mathrm{op}}(\boldsymbol{Q}^2) + G_M^{\mathrm{s},0,m_{\mathrm{s}}^1,\mathrm{wf}}(\boldsymbol{Q}^2), \quad (10)$$

where $G_E^{s,m_s^0}(\boldsymbol{Q}^2)(G_M^{0,m_s^0}(\boldsymbol{Q}^2))$ stands for the $SU(3)$ symmetric part of the strange (flavor-singlet) electric and magnetic form factors, whereas the symmetry-breaking parts $G_E^{s,m_s^1,\mathrm{op}}(\boldsymbol{Q}^2)(G_M^{0,m_s^1,\mathrm{op}}(\boldsymbol{Q}^2))$ and $G_E^{s,m_s^1,\mathrm{wf}}(\boldsymbol{Q}^2)$ $(G_M^{0,m_s^1,\mathrm{wf}}(\boldsymbol{Q}^2))$ correspond to the symmetry breaking in the operator and in the baryon wave functions, respectively. The explicit expressions for the strange vector form factors in eq. (10) are given below. They differ from those of ref. [23] by some numerical constants and by discarding some redundant terms:

$$G_E^{s,m_s^0}(\boldsymbol{Q}^2) = \frac{1}{10}\left(7\mathcal{B}(\boldsymbol{Q}^2) - \frac{\mathcal{I}_1(\boldsymbol{Q}^2)}{I_1} - 6\frac{\mathcal{I}_2(\boldsymbol{Q}^2)}{I_2}\right), \quad (11)$$

$$G_E^{s,m_s^1,\mathrm{op}}(\boldsymbol{Q}^2) = \frac{1}{15}\left((m_0-\bar{m})13 + m_8\frac{5}{\sqrt{3}}\right)\mathcal{C}(\boldsymbol{Q}^2) + m_8\frac{12}{15\sqrt{3}}\left(I_1\mathcal{K}_1(\boldsymbol{Q}^2) - K_1\mathcal{I}_1(\boldsymbol{Q}^2)\right) + m_8\frac{12}{5\sqrt{3}}\left(I_2\mathcal{K}_2(\boldsymbol{Q}^2) - K_2\mathcal{I}_2(\boldsymbol{Q}^2)\right), \quad (12)$$

$$G_E^{s,m_s^1,\mathrm{wf}}(\boldsymbol{Q}^2) = -m_8\left(c_{\overline{10}} + \frac{6\sqrt{3}}{5I_1}c_{27}\right)\mathcal{B}(\boldsymbol{Q}^2) - m_8\frac{1}{5I_1}\left(5\,c_{\overline{10}} - 6\,c_{27}\right)\mathcal{I}_1(\boldsymbol{Q}^2) - m_8\frac{24}{5\sqrt{3}I_2}c_{27}\mathcal{I}_2(\boldsymbol{Q}^2), \quad (13)$$

$$G_M^{s,m_s^0}(\boldsymbol{Q}^2) = \frac{M_\mathrm{N}}{3|\boldsymbol{Q}|}\left\{-\frac{8}{30}\left(\mathcal{Q}_0(\boldsymbol{Q}^2) + \frac{1}{I_1}\mathcal{Q}_1(\boldsymbol{Q}^2) + \frac{1}{6I_2}\mathcal{X}_2(\boldsymbol{Q}^2)\right)S_3 - \frac{1}{15I_1}\mathcal{X}_1(\boldsymbol{Q}^2)\,S_3\right\}, \quad (14)$$

$$G_M^{s,m_s^1,\mathrm{op}}(\boldsymbol{Q}^2) = \frac{M_\mathrm{N}}{3|\boldsymbol{Q}|} \times\left\{-m_8\frac{4}{135}\left(6\mathcal{M}_2(\boldsymbol{Q}^2) - 2\frac{K_2}{I_2}\mathcal{X}_2(\boldsymbol{Q}^2)\right)S_3 - m_8\frac{1}{9}\left(\mathcal{M}_0(\boldsymbol{Q}^2) + \mathcal{M}_1(\boldsymbol{Q}^2) - \frac{1}{3}\frac{K_1}{I_1}\mathcal{X}_1(\boldsymbol{Q}^2)\right)S_3 - m_8\frac{1}{15}\left(\mathcal{M}_0(\boldsymbol{Q}^2) - \mathcal{M}_1(\boldsymbol{Q}^2) + \frac{1}{3}\frac{K_1}{I_1}\mathcal{X}_1(\boldsymbol{Q}^2)\right)S_3 + (m_0-\bar{m})\frac{8}{15}\mathcal{M}_0(\boldsymbol{Q}^2)\,S_3\right\}, \quad (15)$$

$$G_M^{s,m_s^1,\mathrm{wf}}(\boldsymbol{Q}^2) = \frac{M_\mathrm{N}}{3|\boldsymbol{Q}|} \times\left\{-m_8\frac{8}{45}c_{27}\left(\mathcal{Q}_0(\boldsymbol{Q}^2) + \frac{1}{I_1}\mathcal{Q}_1(\boldsymbol{Q}^2) + \frac{2}{I_2}\mathcal{X}_2(\boldsymbol{Q}^2) - \frac{3}{2I_1}\mathcal{X}_1(\boldsymbol{Q}^2)\right)\right\}S_3, \quad (16)$$

The flavor-singlet vector form factors are written as

$$G_E^{0,m_s^0}(\boldsymbol{Q}^2) = \mathcal{B}(\boldsymbol{Q}^2)\,, \quad (17)$$

$$G_E^{0,m_s^1,\mathrm{op}}(\boldsymbol{Q}^2) = \left(2(m_0-\bar{m}) + m_8\frac{3}{10\sqrt{3}}\right)\mathcal{C}(\boldsymbol{Q}^2)\,, \quad (18)$$

$$G_E^{0,m_s^1,\mathrm{wf}}(\boldsymbol{Q}^2) = 0\,, \quad (19)$$

$$G_M^{0,m_s^0}(\boldsymbol{Q}^2) = \frac{M_\mathrm{N}}{|\boldsymbol{Q}|}\frac{\mathcal{X}_1(\boldsymbol{Q}^2)}{I_1}S_3\,, \quad (20)$$

$$G_M^{0,m_s^1,\mathrm{op}}(\boldsymbol{Q}^2) = \frac{M_\mathrm{N}}{|\boldsymbol{Q}|}\frac{m_8\sqrt{3}}{15} \times\left(6\mathcal{M}_1(\boldsymbol{Q}^2) - 2\frac{K_1}{I_1}\mathcal{X}_1(\boldsymbol{Q}^2)\right)S_3\,, \quad (21)$$

$$G_M^{0,m_s^1,\mathrm{wf}}(\boldsymbol{Q}^2) = 0\,, \quad (22)$$

where the coefficients like $c_{\overline{10}}$ are known from the $SU(3)$ algebra, the I_1 etc. are moments of ineria whose expressions can be found in ref. [30]. The other quantities like $\mathcal{I}_1(\boldsymbol{Q}^2)$ are explicitely given in appendix A.

3 Results and discussion

We present now the results obtained from the χQSM. A detailed description on numerical methods is presented in refs. [17, 29]. The parameters of the model are the constituent-quark mass M, the current quark mass m_u, the cut-off Λ of the proper-time regularization, and the strange quark mass m_s. These parameters are not free but are adjusted to independent observables in a very clear way (in fact this was done many years ago): The Λ and the m_u are adjusted for a given M in the mesonic sector. The physical pion mass $m_\pi = 139$ MeV and the pion decay constant $f_\pi = 93$ MeV are reproduced by these parameters. The strange-quark mass is chosen to be $m_\mathrm{s} = 180$ MeV throughout the present work. The remaining parameter M is varied from 400 MeV to 450 MeV. The value of 420 MeV, which for many years is known to produce the best fit to many baryonic observables [17], is selected for our final result in the baryonic sector. The magnetic moments of the proton and neutron in the symmetry-conserving quantization are: $\mu_\mathrm{p} = 1.77\,\mu_\mathrm{N}$ and $\mu_\mathrm{n} = -1.20\,\mu_\mathrm{N}$, respectively. Compared to the experimental data, they are underestimated by 35%.

We always assume isospin symmetry. Actually with this formalism we obtained the results (within the admittedly large experimental errors) in fairly good agreement with the data of SAMPLE and HAPPEX.

The formalism of the χQSM has been applied frequently to $SU(3)$ baryons. In the present case, where explicitly a strange quantity is considered, one meets a problem concerning the asymptotic behavior of the kaon field. While in $SU(2)$ the soliton incorporates the asymptotic pion behavior $\exp(-\mu r)/r$ with $\mu = m_\pi$ in a natural way,

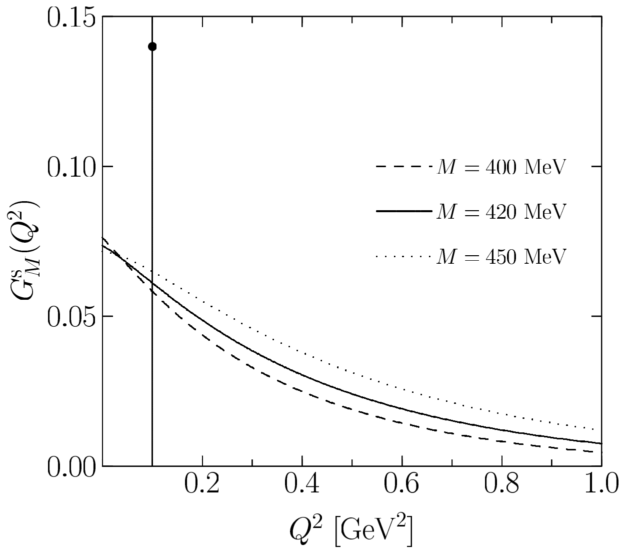

Fig. 1. The dependence of the strange magnetic form factor as a function of Q^2 on the constituent-quark mass with the pion asymptotic tail ($\mu = 140$ MeV). The solid curve is for $M = 420$ MeV, the dashed one for 400 MeV, and the dotted one for 450 MeV. The strange quark mass is $m_{\rm s} = 180$ MeV. The experimental data are taken from SAMPLE [11]. The preferred curve is the one for $M = 420$ MeV.

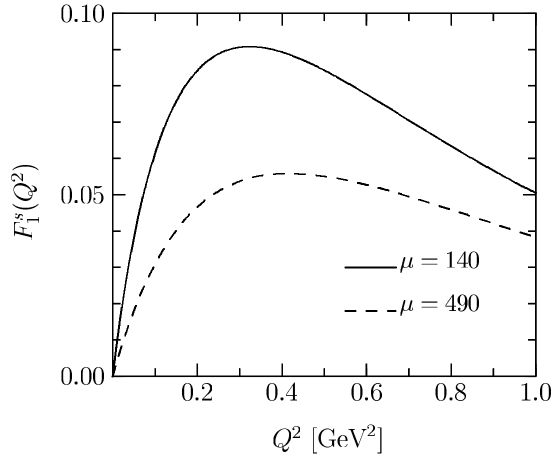

Fig. 2. The form factor $F_1^{\rm s}$ as a function of Q^2. The solid curve and dashed one represent the results for the kaon ($\mu =$ 490 MeV) and pion ($\mu = 140$ MeV) asymptotic tails, respectively. The constituent-quark mass is $M = 420$ MeV.

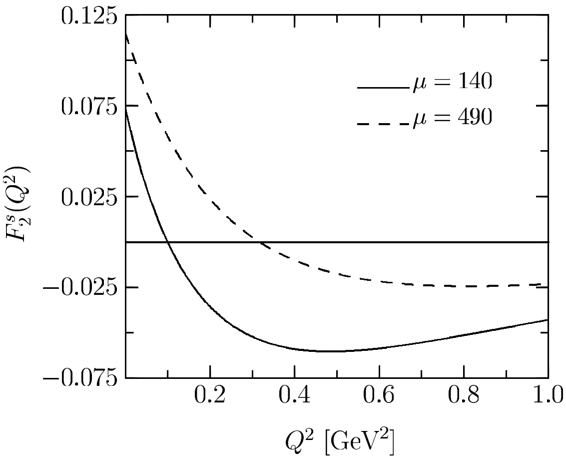

Fig. 3. The form factor $F_2^{\rm s}$ (in physical n.m.) as a function of Q^2. The solid curve and dashed one represent the results for the kaon ($\mu = 490$ MeV) and pion ($\mu = 140$ MeV) asymptotic tails, respectively. The constituent-quark mass is $M = 420$ MeV.

the construction of the $SU(3)$ hedgehog by Witten's embedding causes all other Goldstone bosons to share the same asymptotic behavior. This, however, contradicts the common belief that the asymptotic form of the kaon field is given by $\exp(-\mu r)/r$ with $\mu = m_{\rm K}$. Therefore, in our procedure, there is some sort of systematic error which we have to estimate. We do this described in ref. [26], performing two separate calculations, first by choosing the parameter $\bar{m}$ in the one-body Dirac Hamiltonian with the background meson fields such that the $SU(3)$ calculation yields a pionic tail for all the solitonic profiles ($\mu = m_\pi$), and second, by selecting $\bar{m}$ in order to get a kaonic tail ($\mu = m_{\rm K}$). In both cases we compensate by modifying the perturbative collective treatment of $m_{\rm s}$ (or m_8) by subtracting the corresponding term. Altogether we get for each purely strange contribution to an observable two values the differences of which gives a measure for the systematic error of our solitonic calculation (for the up and down part of an observable we always use the Yukawa mass $\mu = m_\pi$). To get a feeling for the dependence of our results on the other parameters of the model, we also present results for various constituent-quark masses M (always yielding a correct $f_\pi = 93\,\text{MeV}$ and $m_\pi = 139\,\text{MeV}$, of course).

The magnetic strange form factor $G_M^{\rm s}(Q^2)$ for three different values of M is shown in fig. 1 with the pionic asymptotics. This is a typical case such that altogether the effect of the variation of M is not very important and smaller than the effect of having different Yukawa tails. This qualitative feature is true for the electric strange form factors as well. Thus, we consider only the results of our model with $M = 420$ MeV, since it has been shown in several calculations [17] that many other baryonic observables are reproduced well.

The figures for the form factors of the present calculations have been published already in ref. [26]. For completeness, we present here the strange Dirac and Pauli form factors in figs. 2, 3 with kaon and pion tails, resepctively. They will be suitable for a direct comparison with the results of the A4 experiment which will soon come out.

In table 1 we display the prediction of the χQSM for the G0 experiment. Presented is the combination of the strange vector form factors $G_E^{\rm s} + \beta G_M^{\rm s}$. Here, β is defined as

$$\beta(Q^2, \theta) \;=\; \frac{\tau G_M^{\rm p\gamma}}{\epsilon G_E^{\rm p\gamma}}, \tag{23}$$

where $\tau = Q^2/(4M_{\rm N}^2)$ and $\epsilon = [1 + 2(1+\tau)\tan^2(\theta/2)]^{-1}$ and the $G_M^{\rm p\gamma}$ and $G_E^{\rm p\gamma}$ are taken from the experiment. For smaller Q^2 values, $G_E^{\rm s} + \beta G_M^{\rm s}$ is rather sensitive to which tail we use. For example, the result at $Q^2 = 0.16$ GeV^2 shows 15 and 50% difference at $\theta = 10^\circ$ and $\theta = 108^\circ$,

Table 1. Strange form factors: The prediction for the G0 experiment. The constituent-quark mass M is chosen to be 420 MeV. The range represents two different results with the pion and kaon tails, respectively, indicating the systematic error of the model.

	$\theta = 10^\circ$		$\theta = 108^\circ$	
Q^2 (GeV^2)	β	$G_E^s + \beta G_M^s$ ($\mu = m_\pi \sim m_K$)	β	$G_E^s + \beta G_M^s$ ($\mu = m_\pi \sim m_K$)
0.16	0.13	$0.09 \sim 0.05$	0.63	$0.11 \sim 0.09$
0.24	0.20	$0.10 \sim 0.06$	0.99	$0.14 \sim 0.11$
0.325	0.26	$0.11 \sim 0.07$	1.31	$0.14 \sim 0.13$
0.435	0.35	$0.11 \sim 0.07$	1.81	$0.15 \sim 0.14$
0.576	0.47	$0.10 \sim 0.07$	2.49	$0.14 \sim 0.14$
0.751	0.61	$0.08 \sim 0.06$	3.35	$0.12 \sim 0.13$
0.951	0.81	$0.07 \sim 0.06$	4.62	$0.11 \sim 0.12$

Table 2. Singlet form factors: The prediction for the G0 experiment. The constituent-quark mass M is chosen to be 420 MeV. The range represents two different results with the pion and kaon tails, respectively, indicating the systematic error of the model.

	$\theta = 10^\circ$		$\theta = 108^\circ$	
Q^2 (GeV^2)	β	$G_E^0 + \beta G_M^0$ ($\mu = m_\pi \sim m_K$)	β	$G_E^0 + \beta G_M^0$ ($\mu = m_\pi \sim m_K$)
0.16	0.13	$2.38 \sim 2.53$	0.63	$3.05 \sim 3.20$
0.24	0.20	$2.13 \sim 2.33$	0.99	$3.04 \sim 3.27$
0.325	0.26	$1.90 \sim 2.14$	1.31	$2.91 \sim 3.22$
0.435	0.35	$1.65 \sim 1.92$	1.81	$2.80 \sim 3.21$
0.576	0.47	$1.39 \sim 1.69$	2.49	$2.63 \sim 3.15$
0.751	0.61	$1.13 \sim 1.45$	3.35	$2.39 \sim 3.03$
0.951	0.81	$0.92 \sim 1.24$	4.62	$2.21 \sim 2.96$

Table 3. Strange form factors: The prediction for the A4 experiment. The constituent-quark mass M is chosen to be 420 MeV. The range represents two different results with the pion and kaon tails, respectively, indicating the systematic error of the model.

	$\theta = 35^\circ$		$\theta = 145^\circ$	
Q^2 (GeV^2)	β	$G_E^s + \beta G_M^s$ ($\mu = m_\pi \sim m_K$)	β	$G_E^s + \beta G_M^s$ ($\mu = m_\pi \sim m_K$)
0.10	0.099	$0.07 \sim 0.04$	–	–
0.227	0.22	$0.10 \sim 0.06$	4.07	$0.28 \sim 0.32$
0.47	–	–	8.963	$0.33 \sim 0.42$

respectively, between kaon and pion tails, whereas at $Q^2 = 0.951$ GeV^2 we find 10 to 15% difference. Thus, smaller Q^2 show more sensitivity to the tail. The difference between the results from the kaon and pion tails is comparatively smaller at backward angles. In any case this difference indicates the size of the systematic error of our model.

In table 2 we list the predictions of the singlet form factor $G_E^0 + \beta G_M^0$ for the G0 experiment and in tables 3 and 4 we present, respectively, the predictions of the strange form factor $G_E^s + \beta G_M^s$ and singlet form factor $G_E^0 + \beta G_M^0$ at $Q^2 = 0.227$ GeV^2 for the A4 experiment. In table 5 we list the prediction of the strange form factor for the HAPPEX II experiment, whereas in table 6 we predict the corresponding singlet form factor. Again the difference between the numbers obtained using a pion and also a kaon tail indicates the size of the systematic error of our model.

4 Summary and outlook

In the present work, we have investigated the strange vector form factors G_E^s and G_M^s and flavor singlet vector form factors G_E^0 and G_M^0 within the framework of the $SU(3)$ chiral quark-soliton model, incorporating the symmetry-conserving quantization. The rotational $1/N_c$ and strange quark mass m_s corrections were taken into account. In order to get a feeling for the systematic error of our approach in calculating such a sensitive quantity as a strange form factor, we also have considered two different asymptotic behaviors of the soliton in such a way that the tails of the soliton fall off according to the Yukawa mass of the pion and of the kaon.

We first have examined the dependence of the strange form factors on the constituent-quark mass M which is the only free parameter we deal with. The dependence on M turned out rather mild in general and we chose $M = 420$ MeV for which many other properties of the nucleon and the hyperons are reproduced. We also have predicted the combination of the strange form factors, *i.e.* $G_E^s + \beta G_M^s$ and $G_E^0 + \beta G_M^0$ corresponding to kinematics of three different experiments, that is, the G0, A4, and HAPPEX II experiments.

For the presently used chiral quark-soliton model the derivation of a strange contribution to the electromagnetic form factors of the nucleon is a rather natural thing, since the theory can be considered as a many-body approach with a polarized Dirac sea. In fact, as one finds in

Table 4. Singlet form factors: The prediction for the A4 experiment. The constituent-quark mass M is chosen to be 420 MeV. The range represents two different results with the pion and kaon tails, respectively, indicating the systematic error of the model.

	$\theta = 35°$		$\theta = 145°$	
Q^2 (GeV^2)	β	$G_E^0 + \beta G_M^0$ ($\mu = m_\pi \sim m_{\rm K}$)	β	$G_E^0 + \beta G_M^0$ ($\mu = m_\pi \sim m_{\rm K}$)
0.10	0.099	$2.61 \sim 2.72$	–	–
0.227	0.22	$2.21 \sim 2.40$	4.07	$6.72 \sim 7.05$
0.47	–	–	8.963	$7.91 \sim 9.04$

Table 5. Strange form factors: The prediction for the HAPPEX II experiment. The constituent-quark mass M is chosen to be 420 MeV. The range represents two different results with the pion and kaon tails, respectively, indicating the systematic error of the model.

	$\theta = 6°$	
Q^2 (GeV^2)	β	$G_E^{\rm s} + \beta G_M^{\rm s}$ ($\mu = m_\pi \sim m_{\rm K}$)
0.11	0.09	$0.07 \sim 0.04$

Table 6. Singlet form factors: The prediction for the HAPPEX II experiment. The constituent-quark mass M is chosen to be 420 MeV. The range represents two different results with the pion and kaon tails, respectively, indicating the systematic error of the model.

	$\theta = 0.09°$	
Q^2 (GeV^2)	β	$G_E^0 + \beta G_M^0$ ($\mu = m_\pi \sim m_{\rm K}$)
0.11	0.09	$2.55 \sim 2.62$

other observables of the nucleon, about 5%–10% contribution comes from the strange $s\bar{s}$ excitation of the quark sea [17]. If one compares the present approach with others in the literature, one finds a difference insofar that most of the theories yield a negative strange magnetic moment, whereas the present one produces a slightly positive one [26]. The reason might lie in the fact that the present approach is the only one with quarks in a self-consistent static meson field, with a proper treatment of the symmetries in $SU(3)$ including rotational corrections. In particular, the meson field is closely related to the instanton liquid of the QCD vacuum. So far the approach has been successful in $SU(2)$ and here we have a sensitive test in $SU(3)$. It is planned also to calculate the asymmetries of parity-violating electron scattering directly. For this we need axial-vector form factors calculated in $SU(3)$ which is presently under way.

Note added: While the present paper was in the refereeing process, the A4 Collaboration announced their results [31] for $Q^2 = 0.230(\mathrm{GeV}/c)^2$ and $\theta = 35°$. Apparently our predictions agree within the error bars with their results on $G_E^{\rm s} + 0.225 G_M^{\rm s} = 0.039 \pm 0.034$ or $F_1^{\rm s} + 0.130 F_2^{\rm s} = 0.032 \pm 0.028$.

The authors are grateful to F. Maas for useful discussions. HCK thanks also D. von Harrach and M. Pitt for valuable discussions and comments. AS acknowledges partial financial support from Praxis XXI/BD/15681/98. The work of HCK is supported by the Korea Research Foundation Grant (KRF-2003-041-C20067). The work has also been supported by the BMBF, the DFG, the COSY–Project (Jülich) and POCTI (MCT-Portugal).

Appendix A. Densities

In this appendix, we provide the densities for the strange vector and flavor-singlet form factors given in eqs. (16), (22). We list only those, which are different from the ones in the appendix of ref. [23]. The sums run freely over all single-quark levels including the valence one, except the sum over m_0, which is restricted to negative-energy orbits:

$$\mathcal{C}(\boldsymbol{Q}^2) = N_c \int \mathrm{d}^3 x j_0(Qr)$$

$$\times \int \mathrm{d}^3 y \Bigg[\sum_{n \neq \mathrm{val}} \frac{\Psi_n^\dagger(\boldsymbol{x}) \Psi_{\mathrm{val}}(\boldsymbol{x}) \Psi_n^\dagger(\boldsymbol{y}) \beta \Psi_{\mathrm{val}}(\boldsymbol{y})}{E_n - E_{\mathrm{val}}}$$

$$- \frac{1}{2} \sum_{n,m} \Psi_n^\dagger(\boldsymbol{x}) \Psi_m(\boldsymbol{x}) \Psi_m^\dagger(\boldsymbol{y}) \beta \Psi_n(\boldsymbol{y}) \mathcal{R}_{\mathcal{M}}(E_n, E_m) \Bigg],$$

$$\mathcal{I}_2(\boldsymbol{Q}^2) = \frac{N_c}{4} \int \mathrm{d}^3 x j_0(Qr)$$

$$\times \int \mathrm{d}^3 y \Bigg[\sum_{m^0} \frac{\Psi_{m^0}^\dagger(\boldsymbol{x}) \Psi_{\mathrm{val}}(\boldsymbol{x}) \Psi_{\mathrm{val}}^\dagger(\boldsymbol{y}) \Psi_{m^0}(\boldsymbol{y})}{E_{m^0} - E_{\mathrm{val}}}$$

$$+ \frac{1}{2} \sum_{n,m_0} \Psi_n^\dagger(\boldsymbol{x}) \Psi_{m^0}(\boldsymbol{x}) \Psi_{m^0}^\dagger(\boldsymbol{y}) \Psi_n(\boldsymbol{y}) \mathcal{R}_{\mathcal{I}}(E_n, E_{m^0}) \Bigg],$$

$$\mathcal{K}_2(\boldsymbol{Q}^2) = \frac{N_c}{4} \int \mathrm{d}^3 x j_0(Qr)$$

$$\times \int \mathrm{d}^3 y \Bigg[\sum_{m^0} \frac{\Psi_{m^0}^\dagger(\boldsymbol{x}) \Psi_{\mathrm{val}}(\boldsymbol{x}) \Psi_{\mathrm{val}}^\dagger(\boldsymbol{y}) \beta \Psi_{m^0}(\boldsymbol{y})}{E_{m^0} - E_{\mathrm{val}}}$$

$$+ \frac{1}{2} \sum_{n,m_0} \Psi_n^\dagger(\boldsymbol{x}) \Psi_{m^0}(\boldsymbol{x}) \Psi_{m^0}^\dagger(\boldsymbol{y}) \beta \Psi_n(\boldsymbol{y}) \mathcal{R}_{\mathcal{M}}(E_n, E_{m^0}) \Bigg], \tag{A.1}$$

$$\mathcal{M}_0(\boldsymbol{Q}^2) = N_c \int \mathrm{d}^3x \frac{j_1(Qr)}{r}$$

$$\times \int \mathrm{d}^3y \left[\sum_n \frac{\Psi_n^\dagger(\boldsymbol{x})\gamma_5\{\boldsymbol{r}\times\boldsymbol{\sigma}\}\cdot\boldsymbol{\tau}\Psi_{\mathrm{val}}(\boldsymbol{x})\Psi_{\mathrm{val}}^\dagger(\boldsymbol{y})\beta\Psi_n(\boldsymbol{y})}{E_n - E_{\mathrm{val}}} \right.$$

$$+ \frac{1}{2}\sum_{n,m} \Psi_n^\dagger(\boldsymbol{x})\gamma_5\{\boldsymbol{r}\times\boldsymbol{\sigma}\}\cdot\boldsymbol{\tau}$$

$$\left. \times \Psi_m(\boldsymbol{x})\Psi_m^\dagger(\boldsymbol{y})\beta\Psi_n(\boldsymbol{y})\mathcal{R}_\beta(E_n, E_m) \right], \tag{A.2}$$

The regularization functions in eq. (A.2) are as follows:

$$\mathcal{R}_I(E_n, E_m) = -\frac{1}{2\sqrt{\pi}} \int_0^\infty \frac{\mathrm{d}u}{\sqrt{u}} \phi(u; \Lambda_i)$$

$$\times \left[\frac{E_n e^{-uE_n^2} + E_m e^{-uE_m^2}}{E_n + E_m} + \frac{e^{-uE_n^2} - e^{-uE_m^2}}{u(E_n^2 - E_m^2)} \right],$$

$$\mathcal{R}_{\mathcal{M}}(E_n, E_m) = \frac{1}{2} \frac{\mathrm{sgn}(E_n) - \mathrm{sgn}(E_m)}{E_n - E_m},$$

$$\mathcal{R}_{\mathcal{N}}(E_n, E_m) = \frac{1}{2} \frac{\mathrm{sgn}(E_n) - \mathrm{sgn}(E_m)}{|E_n| + |E_m|}, \tag{A.3}$$

where the cutoff function $\phi(u;\Lambda_i) = \sum_i c_i \theta\left(u - \frac{1}{\Lambda_i^2}\right)$ is fixed by reproducing the pion decay constant and other mesonic properties [17].

References

1. J. Ashman *et al.*, Nucl. Phys. B **328**, 1 (1989).
2. B. Adeva *et al.*, Phys. Lett. B **302**, 533 (1993).
3. D. Adams *et al.*, Phys. Lett. B **329**, 399 (1994).
4. P.L. Anthony *et al.*, Phys. Rev. Lett. **71**, 959 (1993).
5. K. Abe *et al.*, Phys. Rev. Lett. **75**, 25 (1995).
6. J. Gasser, H. Leutwyler, M.E. Sainio, Phys. Lett. B **253**, 252 (1991).
7. R.L. Jaffe, Phys. Lett. B **229**, 275 (1989).
8. D.B. Kaplan, A. Manohar, Nucl. Phys. B **310**, 527 (1988).
9. SAMPLE Collaboration (B. Mueller *et al.*), Phys. Rev. Lett. **78**, 3824 (1997).
10. SAMPLE Collaboration (D.T. Spayde *et al.*), Phys. Lett. B **583**, 79 (2004), arXiv:nucl-ex/0312016.
11. SAMPLE Collaboration (R. Hasty *et al.*), Science **290**, 2117 (2000).
12. Particle Data Group (D.E. Groom *et al.*), Eur. Phys. J. C **15**, 1 (2000).
13. HAPPEX Collaboration (K.A. Aniol *et al.*), Phys. Lett. B **509**, 211 (2001).
14. W. Koepf, E.M. Henley, S.J. Pollock, Phys. Lett. B **288**, 11 (1992); N.W. Park, J. Schechter, H. Weigel, Phys. Rev. D **43**, 869 (1991); N.W. Park, H. Weigel, Nucl. Phys. A **541**, 453 (1992); T.D. Cohen, H. Forkel, M. Nielsen, Phys. Lett. B **316**, 1 (1993); M.J. Musolf, M. Burkardt, Z. Phys. C **61**, 433 (1994); H. Forkel, M. Nielsen, X. Jin, T.D. Cohen, Phys. Rev. C **50**, 3108 (1994); M.J. Musolf *et al.*, Phys. Rep. **239**, 1 (1994); H. Weigel, A. Abada, R. Alkofer, H. Reinhardt, Phys. Lett. B **353**, 20 (1995); D.B. Leinweber, Phys. Rev. D **53**, 5115 (1996); H. Forkel, Phys. Rev.C **56**, 510 (1997); S.T. Hong, B.Y. Park, D.P. Min, Phys. Lett. B **414**, 229 (1997); H.-Ch. Kim, M. Praszalowicz, M.V. Polyakov, K. Goeke, Phys. Rev. D **58**, 114027 (1998).
15. D.H. Beck, B.R. Holstein, Int. J. Mod. Phys. E **10**, 1 (2001).
16. D.H. Beck, R.D. McKeown, Annu. Rev. Nucl. Part. Sci. **51**, 189 (2001).
17. C.V. Christov, A. Blotz, H.-Ch. Kim, P. Pobylitsa, T. Watabe, Th. Meissner, E. Ruiz Arriola, K. Goeke, Prog. Part. Nucl. Phys. **37**, 91 (1996).
18. R. Alkofer, H. Reinhardt, H. Weigel, Phys. Rep. **265**, 139 (1996).
19. D. Diakonov, V. Petrov, P. Pobylitsa, M.V. Polyakov, C. Weiss, Nucl. Phys. B **480**, 341 (1996).
20. V.Y. Petrov, P.V. Pobylitsa, M.V. Polyakov, I. Bornig, K. Goeke, C. Weiss, Phys. Rev. D **57**, 4325 (1998).
21. K. Goeke, M.V. Polyakov, M. Vanderhaeghen, Prog. Part. Nucl. Phys. **47**, 401 (2001).
22. D. Diakonov, V. Petrov, M.V. Polyakov, Z. Phys. A **359**, 305 (1997).
23. H.-Ch. Kim, T. Watabe, K. Goeke, Nucl. Phys. A **616**, 606 (1997).
24. T. Watabe, K. Goeke, Nucl. Phys. A **629**, 152C (1998).
25. M. Praszałowicz, T. Watabe, K. Goeke, Nucl. Phys. A **647**, 49 (1999).
26. A. Silva, H.-Ch. Kim, K. Goeke, Phys. Rev. D **65**, 014016 (2002); **66**, 039902 (2002)(E).
27. F.E. Maas, Eur. Phys. J. A **17**, 339 (2003).
28. D. Diakonov, V.Y. Petrov, P.V. Pobylitsa, Nucl. Phys. B **306**, 809 (1988).
29. H.-Ch. Kim, A. Blotz, M.V. Polyakov, K. Goeke, Phys. Rev. D **53**, 4013 (1996).
30. A. Blotz, D. Diakonov, K. Goeke, N.W. Park, V. Petrov, P.V. Pobylitsa, Nucl. Phys. A **555**, 765 (1993).
31. A4 Collaboration (F.E. Maas *et al.*), Phys. Rev. Lett. **93**, 022002 (2004), arXiv:nucl-ex/0401019.